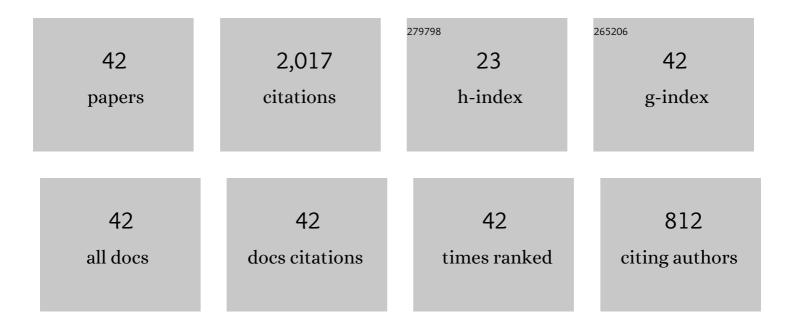
## Behzad Nayebi

List of Publications by Year in descending order

Source: https://exaly.com/author-pdf/9244133/publications.pdf Version: 2024-02-01



#	Article	IF	CITATIONS
1	Effects of carbon additives on the properties of ZrB2–based composites: A review. Ceramics International, 2018, 44, 7334-7348.	4.8	177
2	Characteristics of multi-walled carbon nanotube toughened ZrB 2 –SiC ceramic composite prepared by hot pressing. Ceramics International, 2016, 42, 1950-1958.	4.8	131
3	TEM characterization of spark plasma sintered ZrB2–SiC–graphene nanocomposite. Ceramics International, 2018, 44, 15269-15273.	4.8	103
4	Densification improvement of spark plasma sintered TiB2-based composites with micron-, submicron- and nano-sized SiC particulates. Ceramics International, 2018, 44, 11431-11437.	4.8	100
5	Spark plasma sintering of TiN ceramics codoped with SiC and CNT. Ceramics International, 2019, 45, 3207-3216.	4.8	99
6	Temperature dependence of microstructure evolution during hot pressing of ZrB2–30 vol.% SiC composites. International Journal of Refractory Metals and Hard Materials, 2016, 54, 7-13.	3.8	90
7	Sintering behavior of ZrB2–SiC composites doped with Si3N4: A fractographical approach. Ceramics International, 2017, 43, 9699-9708.	4.8	85
8	Nanoindentation and nanostructural characterization of ZrB2–SiC composite doped with graphite nano-flakes. Composites Part B: Engineering, 2019, 175, 107153.	12.0	84
9	A novel ZrB2–VB2–ZrC composite fabricated by reactive spark plasma sintering. Materials Science & Engineering A: Structural Materials: Properties, Microstructure and Processing, 2018, 731, 131-139.	5.6	82
10	Influence of vanadium content on the characteristics of spark plasma sintered ZrB2–SiC–V composites. Journal of Alloys and Compounds, 2019, 805, 725-732.	5.5	81
11	Fractographical characterization of hot pressed and pressureless sintered AlN-doped ZrB2–SiC composites. Materials Characterization, 2015, 110, 77-85.	4.4	76
12	Microstructure–mechanical properties correlation in spark plasma sintered Ti–4.8Âwt.% TiB2 composites. Materials Chemistry and Physics, 2019, 223, 789-796.	4.0	76
13	Fractographical characterization of hot pressed and pressureless sintered SiAlON-doped ZrB2–SiC composites. Materials Characterization, 2015, 102, 137-145.	4.4	74
14	Reactive hot pressing of ZrB2-based composites with changes in ZrO2/SiC ratio and sintering conditions. Part II: Mechanical behavior. Ceramics International, 2016, 42, 2724-2733.	4.8	71
15	Interfacial phenomena and formation of nano-particles in porous ZrB2–40 vol% B4C UHTC. Ceramics International, 2016, 42, 17009-17015.	4.8	68
16	A fractographical approach to the sintering process in porous ZrB2–B4C binary composites. Ceramics International, 2015, 41, 379-387.	4.8	67
17	Investigation of hot pressed ZrB2–SiC–carbon black nanocomposite by scanning and transmission electron microscopy. Ceramics International, 2019, 45, 16759-16764.	4.8	66
18	Densification and toughening mechanisms in spark plasma sintered ZrB2-based composites with zirconium and graphite additives. Ceramics International, 2020, 46, 13685-13694.	4.8	60

Behzad Nayebi

#	Article	IF	CITATIONS
19	Taguchi analysis on the effect of hot pressing parameters on density and hardness of zirconium diboride. International Journal of Refractory Metals and Hard Materials, 2015, 50, 313-320.	3.8	59
20	Effect of B4C content on sintering behavior, microstructure and mechanical properties of Ti-based composites fabricated via spark plasma sintering. Materials Chemistry and Physics, 2020, 251, 123087.	4.0	44
21	Characterization of ZrB2–TiC composites reinforced with short carbon fibers. Ceramics International, 2020, 46, 23155-23164.	4.8	38
22	Solid solution formation during spark plasma sintering of ZrB2–TiC–graphite composites. Ceramics International, 2020, 46, 2923-2930.	4.8	37
23	Prussian blue-based nanostructured materials: Catalytic applications for environmental remediation and energy conversion. Molecular Catalysis, 2021, 514, 111835.	2.0	24
24	Effect of Zr and C co-addition on the characteristics of ZrB2-based ceramics: Role of spark plasma sintering temperature. Ceramics International, 2020, 46, 24975-24985.	4.8	23
25	Boron nitride-palladium nanostructured catalyst: efficient reduction of nitrobenzene derivatives in water. Nano Express, 2020, 1, 030012.	2.4	21
26	Characteristics of dynamically formed oxide films on molten aluminium. International Journal of Cast Metals Research, 2012, 25, 270-276.	1.0	20
27	Characteristics of dynamically formed oxide films in aluminum–calcium foamable alloys. Journal of Alloys and Compounds, 2016, 655, 433-441.	5.5	20
28	Characteristics of dynamically-formed surface oxide layers on molten zinc–aluminum alloys: A multimodality approach. Thin Solid Films, 2018, 667, 34-39.	1.8	16
29	Spark plasma sintering of TiB2-based ceramics with Ti3AlC2. Ceramics International, 2021, 47, 11929-11934.	4.8	16
30	Nanostructural and nanoindentation characterization of ZrB2 ceramics toughened with in-situ synthesized ZrC. International Journal of Refractory Metals and Hard Materials, 2021, 94, 105391.	3.8	15
31	Nanostructural approach to the thickening behavior and oxidation of calcium-stabilized aluminum foams. Materials Chemistry and Physics, 2018, 220, 351-359.	4.0	12
32	Mechanochemical characteristics of Ca-added Mg-based alloys: A multimodality approach. Materials Characterization, 2020, 167, 110475.	4.4	12
33	Phase transformation in spark plasma sintered ZrB2–V–C composites at different temperatures. Ceramics International, 2020, 46, 9415-9420.	4.8	11
34	A nanostructural approach to the interfacial phenomena in spark plasma sintered TiB2 ceramics with vanadium and graphite additives. Composites Part B: Engineering, 2021, 222, 109069.	12.0	10
35	A novel ZrB2-based composite manufactured with Ti3AlC2 additive. Ceramics International, 2021, 47, 817-827.	4.8	8
36	Toughening of ZrB2-based composites with in-situ synthesized ZrC from ZrO2 and graphite precursors. Journal of Science: Advanced Materials and Devices, 2021, 6, 42-48.	3.1	8

Behzad Nayebi

#	Article	IF	CITATIONS
37	Deformation, Cracking and Fracture Behavior of Dynamically-Formed Oxide Layers on Molten Metals. Metals and Materials International, 2021, 27, 1701-1712.	3.4	8
38	Kinetics of crystallization in 13.2Li2O-67.6SiO2-14.49Al2O3-3.3TiO2-0.4BaO-0.97ZnO glass ceramic powder: Part I: A model-free vs. model-fitting approach. Ceramics International, 2019, 45, 8856-8865.	4.8	7
39	Structural and Magnetic Properties of Co1â^'x Mg x Fe2 O 4 Nanoparticles Synthesized by Microwave-Assisted Combustion Method. Journal of Superconductivity and Novel Magnetism, 2017, 30, 1801-1805.	1.8	5
40	Role of carbon morphology on the synthesizability of ZrC during spark plasma sintering of ZrB2–Zr–C composites. Journal of the Taiwan Institute of Chemical Engineers, 2020, 117, 252-256.	5.3	5
41	Reactive spark plasma sintering of ZrB2-TiC composites: Role of nano-sized carbon black additive. Synthesis and Sintering, 2022, 2, 67-77.	1.6	5
42	Formation of Al–Al2O3 core–shell nanosphere chains during electron beam melting of γ-TiAl. Intermetallics, 2021, 136, 107261.	3.9	3